PHASE TRANSFORMATIONS AND MICROSTRUCTURE DEVELOPMENT DURING HEAT TREATMENT OF Mg–Y–Nd(–Mn)–Zn ALLOYS

KEKULE Tomáš, VLACH Martin, KUDRNOVÁ Hana, KODETOVÁ Veronika, SMOLA Bohumil, STULÍKOVÁ Ivana

Charles University in Prague, Faculty of Mathematics and Physics, Ke Karlovu 5, 121 16 Praha 2, Czech Republic, EU

Abstract

The aim of this work was to investigate and compare microstructure changes in squeeze cast heat treated Mg–2Y–1Nd–1Zn (WEZ211) and Mg–3Y–2Nd–1Zn–1.5Mn (WEZM3211) alloys. The WEZM3211 alloy was isochronally heat treated in 30 °C/30 min steps from room temperature up to 510 °C, the WEZ211 alloy was first isochronally heat treated in steps of 20 °C/20 min up to 440 °C, quenched and isochronally heat treated again. Phase transformations were investigated by several methods: electrical resistivity was measured after each heating step; transmission electron microscopy was performed in selected states; differential scanning calorimetry was realized in the temperature range 20 °C – 510 °C. Electrical resistivity curve of the WEZM3211 alloy exhibits a slight decrease around annealing temperature 150 °C and the main drop in the temperature range 240 °C – 330 °C. This drop can be ascribed mainly to two precipitation processes – formation of thin basal plates of γ´´ phase and subsequently prismatic plates of equilibrium β phase. After annealing at higher temperatures oval particles containing Mn, Y were observed. Electrical resistivity of the WEZ211 alloy shows two decreases connected with formation and development of thin basal plates of γ´phase and ordered γ phase of 14H type.

Keywords: Mg–Y–Nd–Mn–Zn alloys, phase transformations, microstructure development, electrical resistivity

1. INTRODUCTION

Mg alloys with a small addition of rare earth elements (RE) are still in focus of research interests due to specific properties (e. g. [1, 2]) that enable use these alloys not only in traditional fields such as in transport industry but these alloys seem to be promising materials for use in medicine as bearing biodegradable implants. Magnesium itself exhibit very low corrosion resistance, especially in electrolytic, aqueous environments such as in human body. Because of this fact suitable addition in Mg is required to improve corrosion resistance and thus prevent implant to lose mechanical integrity too soon [3]. It is known that appropriate amount of RE including yttrium and scandium contributes to significant improvement of corrosion resistance [4]. The main effect of Zn addition in Mg–RE alloys is a significant decrease of stacking fault energy and precipitation of planar phases parallel to $(0001)_{\alpha\text{-Mg}}$ plane connected with this effect [1]. Mg–Y based alloys with low Zn addition often exhibit ordered structures either in as cast states or after heat treatment. The 18R and 14H long period ordered structures (LPSO) were observed Mg–Y–Zn [5], Mg–Gd (–Y)–Zn [6, 7], Mg–Dy–Zn, Mg–Ho–Zn and Mg–Er–Zn alloys [8]. Zinc has antiseptic effect in human body and up to ~ 6 wt.% is suggested as a suitable addition to Mg alloys designed for biodegradable implants [9]. Easily absorption in vivo was proven for Mg with ~ 1 wt.% Zn and ~ 1 wt.% Mn [10].

This work is focused on investigation of Mg–2Y–1Nd–1Zn (in wt.%, further WEZ211) and Mg–3Y–2Nd–1Zn–1.5Mn (in wt.%, further WEZM3211) alloys and their microstructure development during isochronal annealing.

2. EXPERIMENTAL PROCEDURE

Two alloys were squeeze cast under a protective gas atmosphere of Ar + 1% SF_6. The isochronal annealing response of relative electrical resistivity changes in as cast WEZ211 alloy, resp. as cast WEZM3211 alloy was determined in the range 20 °C – 440 °C [11], resp. 20 °C – 510 °C [12]. Isochronal annealing was carried out in steps of 20 °C/20 min in the WEZ211 and 30 °C/30 min in the WEZM3211 alloy followed by quenching. This treatment was performed in a stirred oil bath up to 240 °C and the specimen was quenched into liquid nitrogen after each annealing step. Specimens wrapped in a steel foil were heat treated in a furnace at higher temperatures and each heating was followed by water quenching. The H-shaped specimens machined to dimensions of cca 1x8x70 mm^3 were used for resistivity measurements at 77 K after each heating step. Relative electrical resistivity changes $\Delta\rho/\rho_0$ were obtained within an accuracy of 10^{-4}. Electrical resistivity was measured by means of the dc four-point method with a dummy specimen in series. The influence of parasitic thermoelectromotive force was suppressed by current reversal. The WEZ211 alloy was annealed and electrical resistivity was measured repeatedly the same way after the first treatment. The microstructure investigation was realized using transmission electron microscopy (TEM) and electron diffraction (ED) in JEOL JEM 2000FX electron microscope. An analysis of phases precipitated out was also supported by energy dispersive X-ray microanalysis (EDS) by BRUKER microanalyzer. Calorimetrical measurements were performed in the NETZSCH DSC 200 F3 Maia calorimeter at constant heating rates of 1 to 20 K/min under a flowing N_2 gas atmosphere.

3. RESULTS AND DISCUSSION

3.1 Microstructure of initial states

The major phase in as cast WEZ211 and WEZM3211 alloys is the α-Mg matrix. Grain boundaries in both alloys are decorated by grain boundary eutectic (GBE) or by particles of the GBE constituent phase which has fcc structure isomorphic with that of primary Mg_3Nd phase (Fig. 1). Particles and structural units of LPSO 14 H phase are noticeable near GBE in WEZM3211 alloy. Grain interior structure exhibits relatively dense planar features with attributes of stacking faults (SF) in both alloys (Fig. 2). Figure 3 shows microstructure of the WEZ211 alloy after the first isochronal annealing up to 440 °C and quenching – initial state of the presented study.

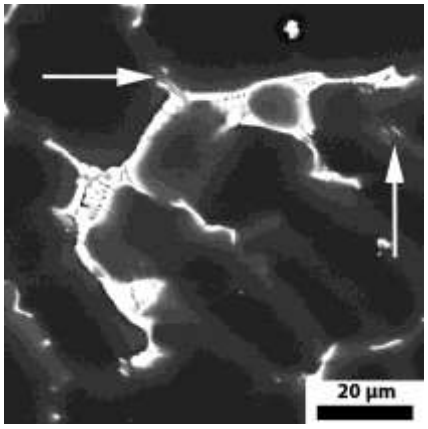

Fig. 1 Grain boundary eutectic and particles of 14H LPSO (marked with arrows) phase in as cast WEZM3211 alloy

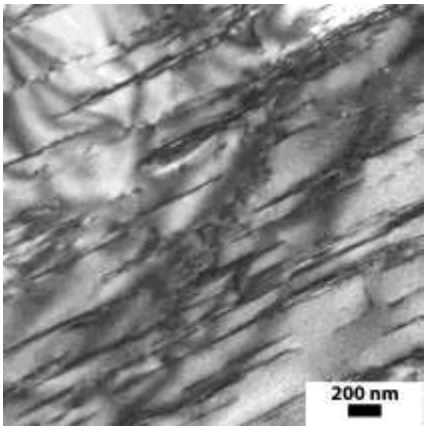

Fig. 2 Planar features parallel to α-Mg basal plain in as cast WEZM3211 alloy

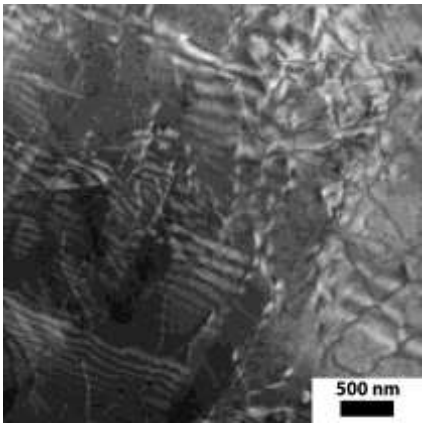

Fig. 3 Microstructure of WEZ211 alloy after preliminary isochronal annealing up to 440 °C

Long and short ribbons of planar features showing SFs image attributes are visible together with dense dislocation distribution. Short ribbons in WEZ211 alloy can represent intrinsic stacking faults similar to those observed in Mg–8Y–2Zn solution treated alloy [1, 13]. Long ribbons in both alloys are most probably structural units of long period ordered structure (LPSO) 14H also observed in solution treated Mg–8Y–2Zn alloy [13] and developing in Mg–6Gd–1Zn alloy during isothermal ageing at 250 °C [1, 6].

3.2 Development during isochronal annealing

Electrical resistivity of the WEZ211 alloy during repeated isochronal annealing from room temperature up to 440 °C decreases up to annealing temperature 180 °C, this decrease is followed by a slight increase up to 280 °C and subsequent second decrease up to annealing temperature 340 °C where the resistivity minimum is reached. Resistivity increases on annealing at higher temperatures and the final value at annealing temperature 440 °C is about 5 % above the initial state. This increase is slowed down between temperatures 340 °C and 380 °C (Fig. 4).

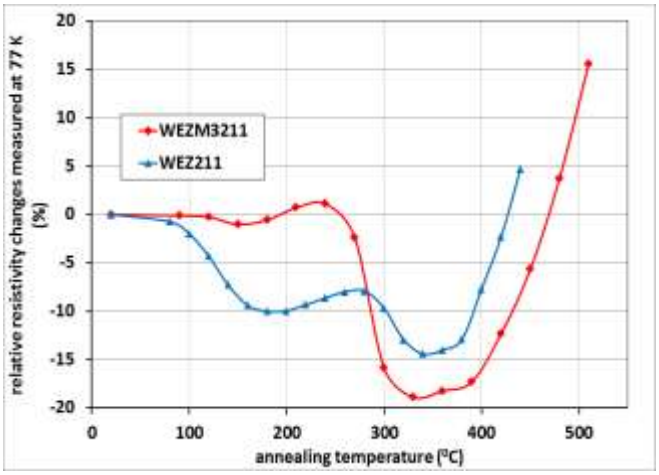

Fig. 4 Electrical resistivity development of WEZ211 and WEZM3211 during isochronal annealing

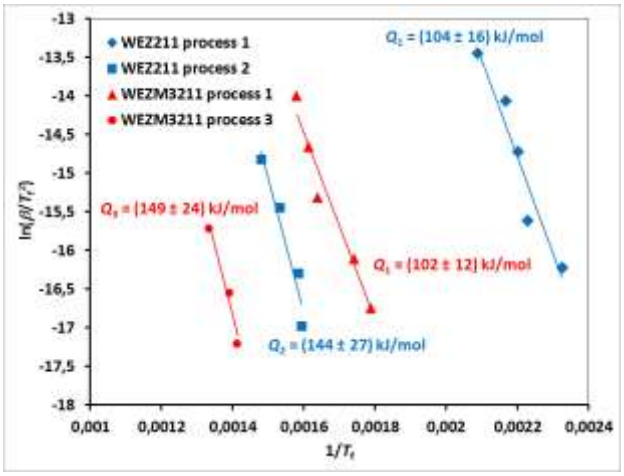

Fig. 5 Kissinger plot for the WEZ211 and WEZM3211 alloy

TEM revealed a changed character of planar features after annealing up to 180 °C – tangled narrow ribbons can be stacking faults bounded by partial Shockley dislocation; long and short ribbons bounded also by dislocations are most probably plates of γ´ phase (hcp, a = 0.32 nm, c = 0.78 nm, $(0001)_{\alpha}$ plate) with composition Mg(Y, Nd)Zn (Fig. 6) [1, 13]. As the majority of alloying elements is in the GBE and grain boundary phases the volume fraction increase of γ´ phase would not be high but sufficient to the resistivity decrease observed.

A slight increase of resistivity between annealing temperatures 180 °C and 260 °C which is caused by increase of solute atoms content in the α-Mg matrix can be ascribed to a partial dissolution of γ´ plates.

Decrease of the solute atoms content in the matrix due to precipitation of another secondary phase is the cause of resistivity decrease with minimum after annealing at 340 °C. Figure 7 shows increased density of planar basal features which is confirmed by stronger intensity streaks observed in SAED. $[41\text{-}50]_{\alpha\text{-Mg}}$ zone SAED (Fig. 8) exhibits extra reflection spots in position 1/7 $(0002)_{\alpha\text{-Mg}}$ spot which corresponds to the position of (0002) reflection of 14H hexagonal LPSO phase [1, 13, 14]. Thus this resistivity decrease is probably response to the formation of γ phase (ordered hcp, 14H, a = 1.11 nm, c = 3.65 nm, $(0001)_{\alpha}$ plate) reported in Mg–Gd–Zn and Mg–Y–Zn alloys [1, 6].

Microstructure of WEZ211 alloy annealed up to 380 °C exhibits a little lower density of planar features than that after annealing up to 340 °C but probably the majority of features are basal plates of 14H γ phase.

Resistivity increase shows dissolution of planar defects at higher temperatures up to 440 °C. Microstructure is characterized by long planar features which are most probably plates of γ phase 14H similarly to the microstructure of the initial state.

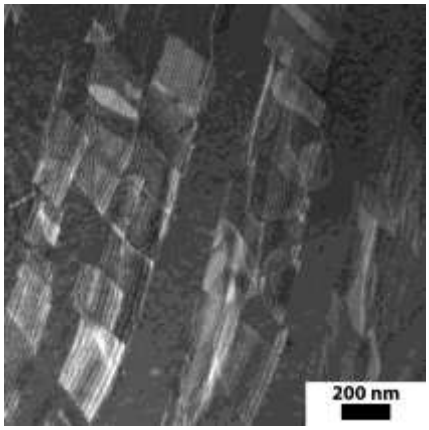

Fig. 6 Planar features and short ribbons of stacking faults in WEZ211 alloy annealed up to 180 °C

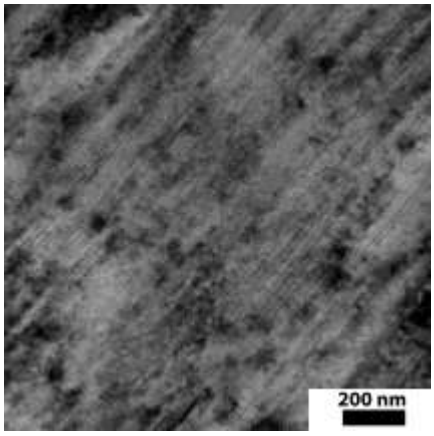

Fig. 7 Planar features in WEZ211 alloy annealed up to 340 °C imaged along $[10\text{-}10]_{\alpha\text{-Mg}}$ direction

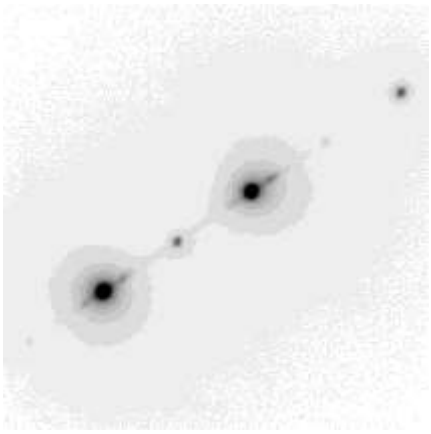

Fig. 8 $[41\text{-}50]_{\alpha\text{-Mg}}$ zone ED patterns of WEZ211 alloy annealed up to 340 °C – extra spots near to primary and strong matrix spot.

Electrical resistivity development of the WEZM3211 alloy (Fig. 4) exhibits insignificant decrease from 90 ºC up to 150 ºC and subsequent increase up to 240 ºC which is followed by resistivity drop up to 330 ºC. Resistivity increase from this minimum is slowed down near 390 ºC by precipitation of another phase. Resistivity value exceeds the initial value about 15 % after annealing at 510 ºC.

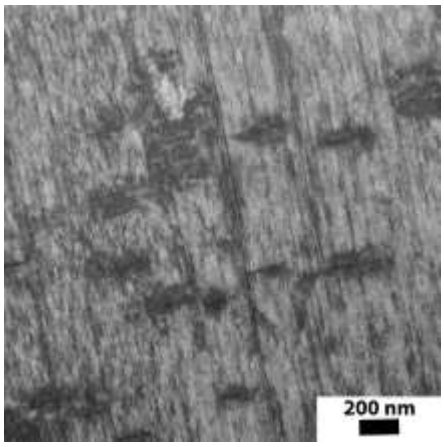

Fig. 9 Thin hexagonal basal plates and prismatic plates of stable β phase in WEZM3211 alloy isochronally annealed up to 330 °C

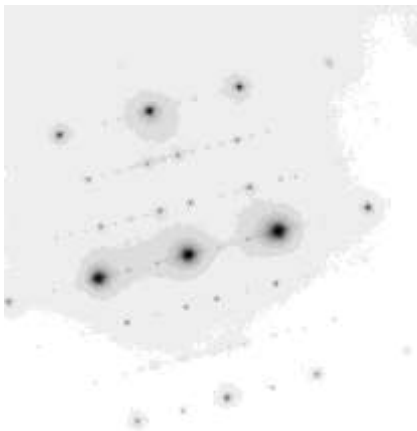

Fig. 10 Overlapping of $[1\text{-}100]_{\alpha\text{-Mg}}$ and $[1\text{-}100]_{\beta}$ zones in ED od of the WEZM3211 alloy annealed up to 330 °C

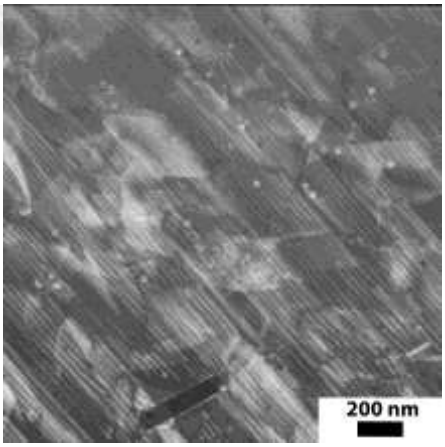

Fig. 11 Planar features and oval particles containing RE and Mn in the WEZM3211 alloy annealed up to 420 °C

Microstructure development of the WEZM3211 alloy during isochronal annealing is completely different than in the WEZ211. Considerable resistivity decrease to its minimum value reached by annealing up to 330 ºC was caused by precipitation of dense distribution of thin basal plates of γ´´ phase or ordered GP zones. Besides of these thin hexagonal basal plates also prismatic plates of equilibrium β phase of the Mg–Y–Nd alloys decomposition sequence, namely $Mg_{14}Nd_2Y$ phase (fcc structure a = 2.20 nm, $\{10\text{-}10\}_{\alpha}$ plate)

isomorphous with Mg_5Gd phase, started to precipitate during annealing up to 330 ºC (Fig. 9, 10). During further isochronal annealing up to 420 ºC the oval particles containing RE and Mn precipitated simultaneously with coarsening of prismatic plates of the equilibrium β phase (Fig. 11). These two precipitation processes slowed down the resistivity increase near annealing temperature 390 ºC (Fig. 4).

The dissolution of thin hexagonal basal plates and their partial transformation to another type of planar defects (γ´ or γ phase) is responsible for the pronounced resistivity increase during annealing at higher temperatures. After annealing up to 480 ºC relatively low density of planar features is situated in grain interiors while an extremely high planar features density was observed in the vicinity of the grain boundary phase particles. Both planar features are most probably structural units of the stable LPSO 14H γ phase known from Mg–Gd–Zn and Mg–Y–Zn alloys [1, 6, 13]. Prismatic plates of the stable β phase also dissolved.

Two exothermic heat effects in both WEZ211 and WEZM3211 alloys can be identified in DSC curves at heating rates 1 K/min – 20 K/min. The temperature position of these effects shifts to higher temperatures with increasing heating rate. Comparing DSC peaks and resistivity decreases it is supposed that the first process in the WEZ211 alloy represents precipitations of γ´ basal plates phase and the second process precipitation of 14H γ phase plates. Development of γ´´ basal plates in the WEZM3211 alloy annealed up to 330 ºC is responsible for the first process observed in DSC. Heat response to β prismatic plates development is very poor and the second peak in DSC curves can be ascribed to precipitation of oval Mn, Y containing particles.

The Kissinger method with the assumption that the peak temperature T_f in DSC curves for individual precipitation processes can be expressed as

$$\ln \frac{\beta}{T_f^2} = -\frac{E}{RT_f} + C, \qquad (1)$$

where C is a constant, E the activation energy of the precipitation process, R the gas constant, β a heating rate and T_f is the peak temperature of the DSC signal, is plotted in Fig. 5.

The values of the activation energy were determined as (104 ± 16) kJ/mol for precipitation of γ´ basal plates, (144 ± 27) kJ/mol for formation of 14H LPSO γ phase plates in the WEZ211 alloy, (102 ± 12) kJ/mol for precipitation of γ´´ phase and (149 ± 24) kJ/mol for rich Mn, Y oval particles development in the WEZM3211 alloy. The activation energies of the γ´ and γ´´ basal plates development are somewhat lower than bulk diffusion energy of Zn in Mg (120 kJ/mol [15]) or Y in Mg (170 kJ/mol - diffusion energy of Y in Mg–Nd–Ag alloy [16]), what is often observed in formation of planar objects. The energy increases if the planar character is lost in formation of the 14H LPSO. The activation energy of precipitation of oval particles in the WEZM3211 corresponds to diffusion energy of Mn [17] (154 kJ/mol) and to that of Y in Mg.

CONCLUSIONS

The main characteristics of microstructure of both alloys in as prepared state are relatively dense planar features parallel to the basal α-Mg plane. Microstructure development of as cast WEZM3211 and WEZ211 formerly subjected to isochronal annealing up 440 ºC is different. The precipitation observed in the WEZ211 is gradually γ´ and γ phase development in the form of planar defects and structural units of 14H LPSO phase, resp. Precipitation, mutual transformation and dissolution of planar features, namely structural units of 14H LPSO γ phase and/or γ´, intrinsic stacking faults and thin hexagonal basal plates of γ´´ phase play a substantial role in the microstructure development of the WEZM3211 alloy. Formation of prismatic plates of the stable β phase (fcc $Mg_{14}Nd_2Y$) and precipitation of oval particles containing RE and Mn also contributes to phase transformations in the process of isochronal annealing performed. Activation energies were determined as (104 ± 16) kJ/mol for precipitation of γ´ basal plates, (144 ± 27) kJ/mol for formation of 14H

LPSO γ phase plates in the WEZ211 alloy, (102 ± 12) kJ/mol for precipitation of γ´´ phase and (149 ± 24) kJ/mol for rich Mn, Y oval particles development in the WEZM3211 alloy.

ACKNOWLEDGEMENTS

The work of Tomáš Kekule and Martin Vlach is a part of activities of the Charles University Research Center "Physics of Condensed Matter and Functional Materials".

REFERENCES

[1] NIE, J. F. Precipitation and hardening in magnesium alloys. Metall. Mater. Trans., A43, 2012, p. 3891-3939.

[2] ČÍŽEK J., PROCHÁZKA I., SMOLA B., STULÍKOVÁ I., VLACH M., OČENÁŠEK V., KULYASOVA O.B., ISLAMGALIEV R.K. Precipitation effects in ultra-fine-grained Mg–RE alloys. International Journal of Materials Research, Vol. 100, Issue 6, 2009, p. 780-784.

[3] YUN YH., DONG Z., YANG D., SCHULZ MJ., SHANOV VN., YARMOLENKO S. et al. Biodegradable Mg corrosion and osteoblast cell culture studies. Mater. Sci. Eng. C, 29, 2009, p. 1814-1821.

[4] NEUBERT V., STULÍKOVÁ I., SMOLA B., BAKKAR A., MORDIKE B.L. Corrosion behaviour of highly creep resistant magnesium-rare-earth-based alloys. Kovove mater., 42, 2004, p. 31-41.

[5] LUO Z. P., ZHANG S. Q. High-resolution electron microscopy on the X-Mg_{12}ZnY phase in a high strength Mg-Zn-Zr-Y magnesium alloy. J. Mater. Sci. Letters 19, 2000, p. 813-815.

[6] NIE J.F., OH-ISHI K., GAO X., HONO K. Solute segregation and precipitation in a creep-resistant Mg–Gd–Zn alloy. Acta Mater. 56, 2008, p. 6061–6076.

[7] HONMA T., OHKUBO T., KAMADO S., HONO K. Effect of Zn additions on the age-hardening of Mg–2.0Gd–1.2Y–0.2Zr alloys. Acta Mater. 55, 2007, p. 4137-4150.

[8] AMIYA K., OHSUNA T., INOUE A. Long-period hexagonal structures in melt-spun Mg97Ln2Zn1 (Ln=lanthanide metal) alloys. Mater. Trans 44, 2003, p. 2151-2156.

[9] ZHANG S., ZHANG X., ZHAO Ch., LI J., SONG Y., XIE Ch., et. al. Research on Mg-Zn alloy as a degradable biomaterial. Acta Biomater. 6, 2010, p. 626 – 640.

[10] XU L., YU G., ZHANG E., PAN F., YANG K. In vivo corrosion behavior of Mg-Mn-Zn alloy for bone implant application. J. Biomed mater. Res. 83A, 2007, p. 703-711.

[11] KEKULE T., VLACH M., CÍSAŘOVÁ H., SMOLA B., STULÍKOVÁ I. Effect of heat treatment on phase transformations in Mg-Y-(Nd)-Zn alloys. In METAL 2012: 21st International Conference on Metallurgy and Materials. Ostrava: TANGER, 2012.

[12] SMOLA, STULÍKOVÁ, PELCOVÁ, ŽALUDOVÁ. The Effect of Zn Addition on Decomposition and Mechanical Properties of Mg-Rare Earth-Mn Alloys. In Magnesium: Proceedings of the 7th International Conference on Magnesium Alloys and Their Applications. Weinheim: Wiley-VCH, 2007.

[13] ZHU Y. M., MORTON A. J., WEYLAND M., NIE J. F. Characterization of planar features in Mg-Y-Zn alloys. Acta Mater., 58, 2, 2010, p. 464-475.

[14] ZHU Y. M., MORTON A. J., NIE J. F. The 18R and 14H long-period stacking ordered structures in Mg–Y–Zn alloys. Acta Mater. 58, 2010, p. 2936-2947.

[15] STLOUKAL I., ČERMÁK J. Diffusion of Zn-65 in AZ91 and in QE22 reinforced by Saffil fibers. Composites Science and Technology, Vol. 68, Issue 2, 2008, p. 417-423.

[16] ČERMÁK J., STLOUKAL I. Mechanism of 88Y diffusion in QE22 alloy. In METAL 2008: 17th International Conference on Metallurgy and Materials. Ostrava: TANGER, 2008.

[17] FUJIKAWA S. I. Diffusion in magnesium. J. Jpn. Inst. Light Met. 42, 1992, p. 822-825.